



TENTH TETRAHEDRON SYMPOSIUM

Register now for live webcasts, interactive chat sessions and access to

NEW  
Experience


Sensors and Actuators A: Physical

Volume 153, Issue 1, 25 June 2009, Pages 114-119

Article

Figures/Tables

References



 PDF (1164 K)

doi:10.1016/j.sna.2009.04.002

 Cite or Link Using DOI

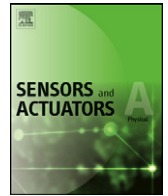
Copyright © 2009 Elsevier B.V. All rights reserved.

## A stiff and flat membrane operated DC contact type RF MEMS switch with low actuation voltage

Jongseok Kim<sup>a, b</sup>, Sangwook Kwon<sup>a</sup>, Heemoon Jeong<sup>a</sup>, Youngtack Hong<sup>a</sup>, Sanghun Lee<sup>a</sup>, Insang Song<sup>a</sup> and Byeongkwon Ju<sup>b</sup>  

<sup>a</sup>Samsung Advanced Institute of Technology, San 14-1, Nongseo-Dong, Giheung-Gu, Youngin-Si, Gyeonggi-Do 449-712, Republic of Korea

<sup>b</sup>Display and Nanosystem Laboratory, College of Engineering, Korea University, Anam-dong, Seong buk-gu, Seoul 136-701, Republic of Korea



## A stiff and flat membrane operated DC contact type RF MEMS switch with low actuation voltage

Jongseok Kim<sup>a,b</sup>, Sangwook Kwon<sup>a</sup>, Heemoon Jeong<sup>a</sup>, Youngtack Hong<sup>a</sup>, Sanghun Lee<sup>a</sup>, Insang Song<sup>a</sup>, Byeongkwon Ju<sup>b,\*</sup>

<sup>a</sup> Samsung Advanced Institute of Technology, San 14-1, Nongseo-Dong, Giheung-Gu, Youngin-Si, Gyeonggi-Do 449-712, Republic of Korea

<sup>b</sup> Display and Nanosystem Laboratory, College of Engineering, Korea University, Anam-dong, Seong buk-gu, Seoul 136-701, Republic of Korea

### ARTICLE INFO

#### Article history:

Received 22 August 2007

Received in revised form 7 March 2009

Accepted 2 April 2009

Available online 10 April 2009

#### Keywords:

RF switch

Stiff membrane

Variable seesaw

### ABSTRACT

RF MEMS switches can be divided into electrostatic, magnetic, thermal, and piezoelectric types by their actuation mechanisms. Most research has focused on the electrostatic actuation types because of these types low power consumption, simple fabrication method, and good RF characteristics. However, these types of switches operate at high voltages compared with the other types. One of the main problems that affect the operation voltages is the bending of the membrane due to an internal stress gradient. To solve this problem, a thick and stiff membrane operated RF MEMS switch has been developed and is presented in this paper. This membrane consists of a flexible spring for an up-down actuation mode at low voltage and a pivot under the membrane for a seesaw mode on-off switch operation. This novel RF MEMS switch has been fabricated, and its RF characteristics measured. The minimum actuation voltage is approximately 10–12 V, the isolation approximately –50 dB, and the insertion loss is approximately –0.25 dB at 2 GHz, respectively. The bending range of the membrane has been measured by using an optical 3D profiler and the height is within 0.2 μm across the 800 μm length membrane. This bending range is uniform across all samples of an entire 4 in. wafer.

© 2009 Elsevier B.V. All rights reserved.

### 1. Introduction

Radio Frequency Micro-Electro-Mechanical Systems (RF MEMS) technology offers good possibilities for realizing a new generation of RF components such as a RF MEMS Switches [1–4]. These switches have many benefits compared with solid state switches in terms of their low insertion losses, negligible power consumptions, good isolations, high power handling capabilities, and excellent linearity characteristics. As a consequence, companies developing RF MEMS switches are making attempt to replace the pin diode, GaAs MESFET, or JFET base semiconductor switches with RF MEMS switches in wireless communication devices, such as multiband selectors and filter banks. Several types of RF MEMS switches have been developed over the last decade [5–8]. Among these switches, the conventional seesaw actuated switches have good isolations and anti-stiction characteristics but they require a high operation voltage in obtaining the required restoring and contact forces. The conventional membrane type switches also have several advantages, such as their low power consumptions,

simple fabrication methods, and good RF characteristics, but they also need a high operation voltage to generate sufficient restoring force and to prevent the stiction of the membrane. Most of these types of switches reported to date, need a high actuation voltage, usually ranging from 20 to 80 V, making them impractical for reconfigurable circuit applications as well as for mobile wireless communication. In this paper, the merits of these two types of switches have been combined, and the operation voltage has been decreased. The membrane with a flexible spring has been designed for reducing the initial actuation voltage, and a pivot has been designed under the membrane for the seesaw mode operation resulting in the low voltage operation. This new concept is known as a “variable pivot seesaw” because as the membrane is actuated downwards it operates in a seesaw-like mode. This concept overcomes the disadvantage of the high voltage characteristics of the conventional seesaw mode actuated switch, which is required for obtaining the necessary restoring and contact forces. Also, a voltage decrease is obtained, comparable to the seesaw type of switches while maintaining high isolation comparable to the membrane type of switches.

The actuation voltage of these membrane operated types of switches can be written as

$$V_p = \left( \frac{8K_s g_0^3}{27\epsilon_0} \right)^{1/2} \quad (1)$$

\* Corresponding author at: Display and Nanosystem Laboratory, College of Engineering, Korea University, Anam-dong, Seong buk-gu, Seoul 136-701, Republic of Korea.

E-mail address: [bkju@korea.ac.kr](mailto:bkju@korea.ac.kr) (B. Ju).

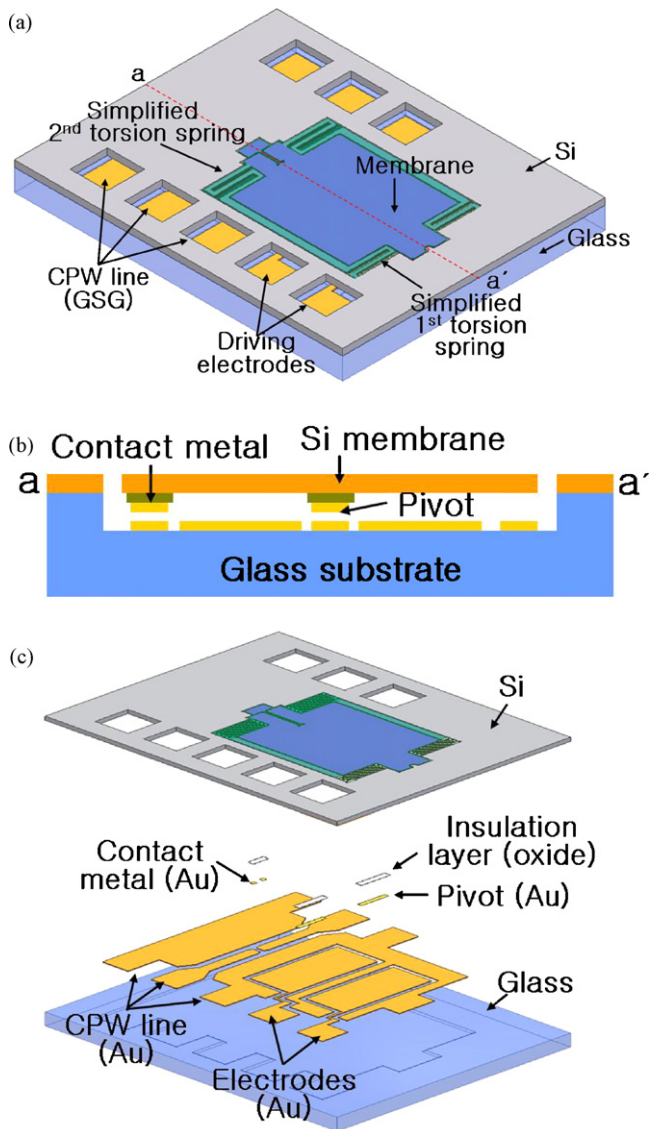


**Fig. 1.** A schematic view of the proposed RF MEMS switch: (a) 3D image of the MEMS switch, (b) Cross-sectional view of a–a’ area, (c) The MEMS switch each layer description.

where,  $V_p$  is the actuation voltage,  $K_s$  is the spring constant,  $\epsilon_0$  is the permittivity of free space and  $g_0$  is the initial gap between the membrane and the electrode. It can be seen from the equation that if this spring constant and permittivity is fixed, the gap between the electrode and membrane is a critical factor affecting the actuation voltage [9]. However, the residual stress during the fabrication process often results in a locally different bending of the membrane, causing a variation in gap width and a requirement for higher driving voltages [10,11]. To solve these problems, single crystalline bulk silicon has been used for the membrane fabrication where there is a low initial stress and it is robust from the bending compared with deposited film type membranes. It is expected that this design will increase the reproducibility and reliability of the purposed switches that utilize this approach.

## 2. Experiment

### 2.1. Design and simulation

Fig. 1 shows schematic views of the proposed RF MEMS switch where a coplanar wave guide (CPW) line has been formed for the

**Table 1**  
The simulation parameters and the pattern dimensions of the proposed design.

Section	Parameter	Figure
Simulation Parameter (Si)	Elastic modulus	168.9 GPa
	Young’s modulus	50.9 GPa
	Poisson’s ratio	0.064
Pattern dimension ( $\mu\text{m}$ )	$W$	1200
	$l$	1500
	$E_{gw}$	1006
	$E_w$	490
	$E_1$	230
	$E_g$	150
	$E_p$	100
	$M_w$	500
	$M_s$	545
	$S_1$	200
	$S_w$	5
	$S_p$	5
$S_{bw}$	30	

RF signal pass, and electrodes for the membrane operation on the glass wafer. The signal line width of the CPW line is  $50\ \mu\text{m}$  and the gap between the signal and the ground line is  $3\ \mu\text{m}$ , initially. The gap of the broken signal lines is  $20\ \mu\text{m}$ . The membrane, with pivot and folded springs for membrane actuation, is formed on the silicon wafer and it is this folded spring that provides the low values for the spring constant in a compact area. The spring constant decreases linearly, with the successive addition of further folded springs [12,13]. The first torsion spring, a spring bar, and a second torsion spring are all connected to each other. The end of the first torsion spring is connected to the anchored silicon and the end of the second torsion spring is connected to the membrane. The spring bar couples the first and second springs. Fig. 2 and Table 1 shows the brief dimensions of the proposed design and the main simulation parameters with the length of one spring line being  $190\ \mu\text{m}$  and its width being  $5\ \mu\text{m}$ . The first torsion spring consists of three meander springs, while the second torsion spring consists of 4.5 meander springs. A pivot is formed under the center of the membrane which is used for the seesaw mode operation when the membrane is actuated downward. The size of each of the pivots is  $150\ \mu\text{m} \times 20\ \mu\text{m}$ . Fig. 3 shows a schematic view of the operating method. Initially, the switch is in the “off” state and the gap between the bottom electrode and the membrane is  $3\ \mu\text{m}$ . When the DC voltage is applied to the contact electrode, the membrane is actuated downward. The contact pad metal connects the broken CPW line and the switching changes to the “on” state. The electrode and membrane have a  $1\ \mu\text{m}$  gap when the switch is in the on state. Because of the  $30\ \mu\text{m}$  thickness membrane and pivot, this very narrow gap is maintained without bending or stiction, making it possible to operate the switch at a very low voltage. When the DC voltage is applied to the restoring electrode, this membrane operates like a seesaw and the switching changes to the “off” state. As long as the DC voltage is applied to the driving electrode or restoring electrode, the switch operates in this seesaw-like mode. To estimate the actuation voltage, the bending of the first and second torsion springs, with an applied bias, has been simulated using the ANSYS program. Fig. 4 shows the simulated results for the structure and springs. When a 5 V DC bias is applied between the bottom electrode and the silicon body, the contact pad moves downwards by  $1.5\ \mu\text{m}$ .

### 2.2. Fabrication and measurement

Fig. 5 shows a fabrication process flow of the proposed switch. The membrane with the spring and pivot was formed on a silicon wafer and the CPW line is fabricated on the cavity of a glass wafer.

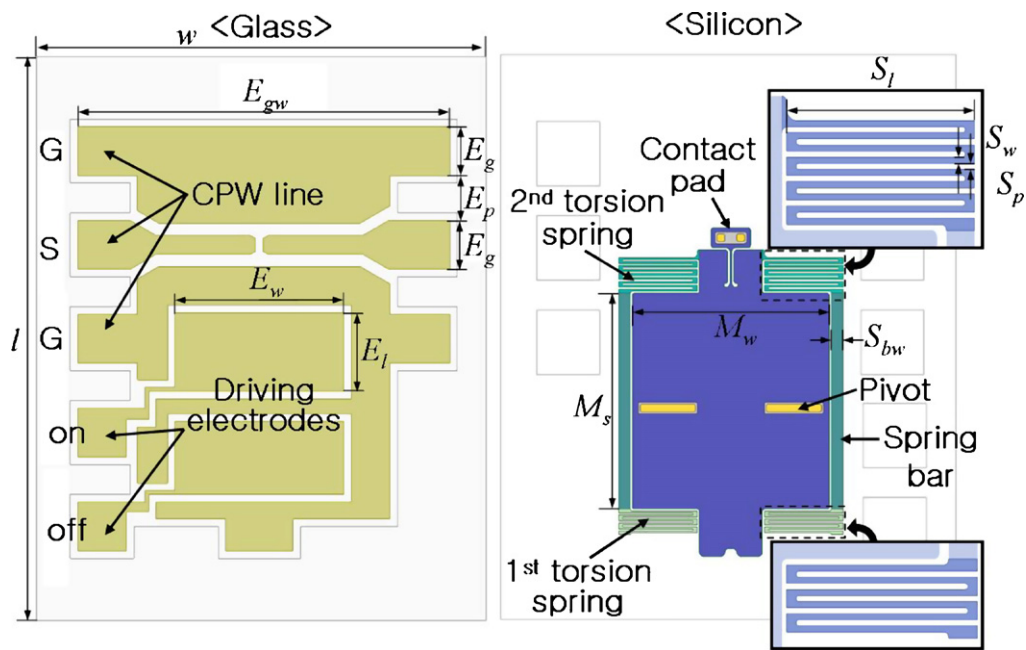


Fig. 2. A top view of the bottom electrode and the backside view of the membrane.

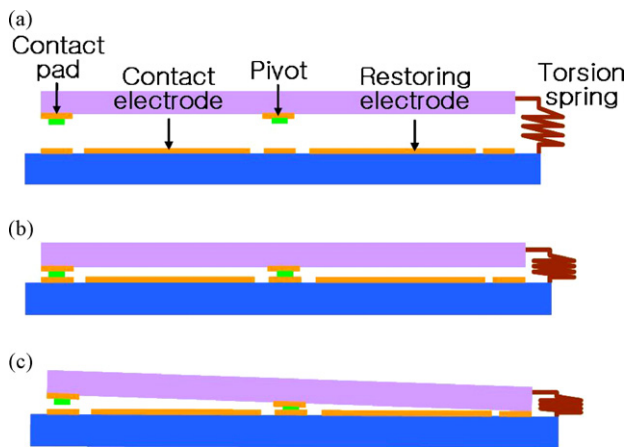


Fig. 3. The simplified operating mode of the proposed RF MEMS switch: (a) The initial “off” state of the MEMS switch, (b) The “on” state of the MEMS switch, (c) The seesaw mode “off” state of the MEMS switch.

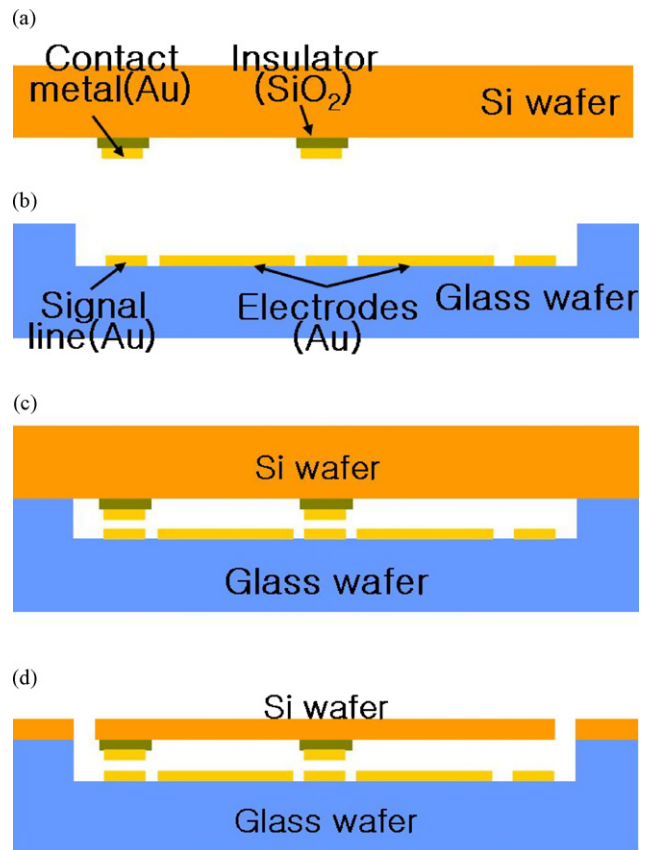


Fig. 5. The fabrication process for the proposed MEMS switch: (a) Insulator and contact pad formation, (b) Cavity and metal pad formation, (c) Si and glass wafer bonding, (d) Si CMP and structure patterning.

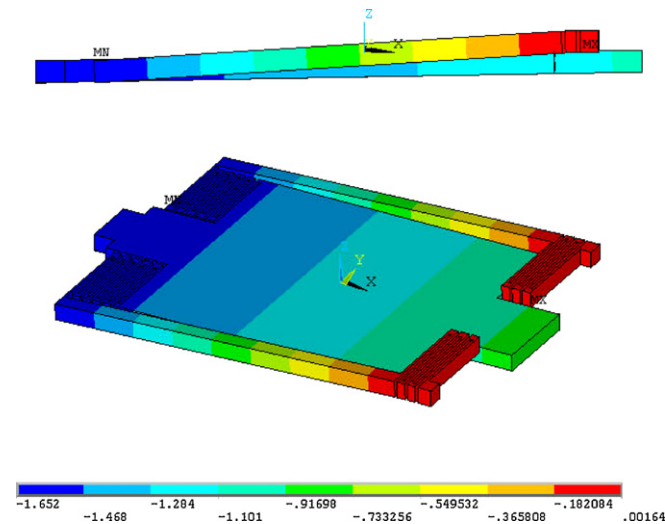


Fig. 4. Simulated results of the membrane structure and springs.

An anodic bonding method has been used to assemble these two wafers [14,15].

The silicon wafer is a p-type (100) with a resistivity of 0.01–0.02 Ωcm. On the Si wafer, 500 nm of thermal oxide is



**Table 2**  
The fabrication parameters of the proposed MEMS switch.

Part	Layer	Materials	Thickness
Si	Insulator	oxide	500 nm
	Contact	Au	500 nm
	Membrane	Si	30 μm
Glass	Cavity	Glass	4.5 μm
	CPW	Au	1.5 μm

deposited to form an insulation layer, and patterned by a wet etch method. To fabricate the contact metal, an Au layer is deposited and patterned by a wet etch method. “Corning 7740 Pyrex” glass wafer is used to minimize the CTE (coefficient of thermal expansion) mismatch problem. Poly-Si is deposited on this glass wafer by using low pressure chemical vapor deposition (LPCVD) equipment. This poly-Si layer is used for the glass etching mask. The deposition temperature of normal poly-Si is 650 °C, but here, the poly-Si is deposited on the glass wafer below 510 °C in order to prevent straining in the glass wafer. The Poly-Si is patterned by using a reactive ion etcher (RIE), and then a cavity of glass is formed by using a buffered oxide etchant (BOE). After the glass etching process, the poly-Si layer is stripped by using a tetramethylammonium hydroxide (TMAH) solution and Au is sputtered on the glass wafer and patterned using Photoresist. The Au CPW line and the electrode pattern are defined by using an Au wet etching process.

After completion of the processing of each of the wafers, the initial cleaning is carried out for the bonding. Surface cleaning is very important because any minor contamination of the surface of the glass, or the Si, can seriously affect the bonding conditions. H<sub>2</sub>SO<sub>4</sub> with H<sub>2</sub>O<sub>2</sub> is used with the HF dipping method for cleaning the surface of the wafers: 1 min dipped in the H<sub>2</sub>SO<sub>4</sub> with H<sub>2</sub>O<sub>2</sub> solution and 10 s dipped in the HF solution. After the dipping process, the Si and glass wafer are bonded by using an anodic bonding method. The advantage of this separate process not only effectively avoids contamination which can be from the sacrificial layer residue, and secures the reliability of the contact metal, but the process is also effective for precision gap control, determined by the metal thickness. The bonding temperature is 380 °C, at a pressure of 100 N and a 600 V DC voltage is applied for 5 min.

After the bonding process, the Si layer is polished until 30 μm remained. The membrane structure is patterned on the polished Si layer and etched by using an inductively coupled plasma reactive ion etcher (ICP-RIE). The structure patterned photoresist is removed by using a dry Asher. Because of thermal stress, a low temperature Asher is used to prevent the bending of the Si springs and the membrane structure. Table 2 presents the fabrication parameters of the proposed switch.

The RF characteristics of the fabricated RF MEMS switch are measured using a HP 8510C vector network analyzer and a Micro-manipulator RF probe station. A ground-signal-ground (G-S-G) type GGB Picoprobe tip is used with a pitch size of the G-S, 250 μm to make the on wafer measurements and a standard short-open-load-through (SOLT) calibration has also been performed using an alumina based substrate with specified planar standards.

**3. Results and discussion**

The bending range of the membrane has been measured by using an optical 3D profiler and a measured image is shown in Fig. 6, where the color variation denotes the height variation; the measurement unit in this figure is a nanometer. The bending range of height is within 0.2 μm across the 800 μm length of the membrane. Fig. 7 shows a measured bending height of 25 samples, randomly selected from top, center, bottom, left and right of the wafer. It has

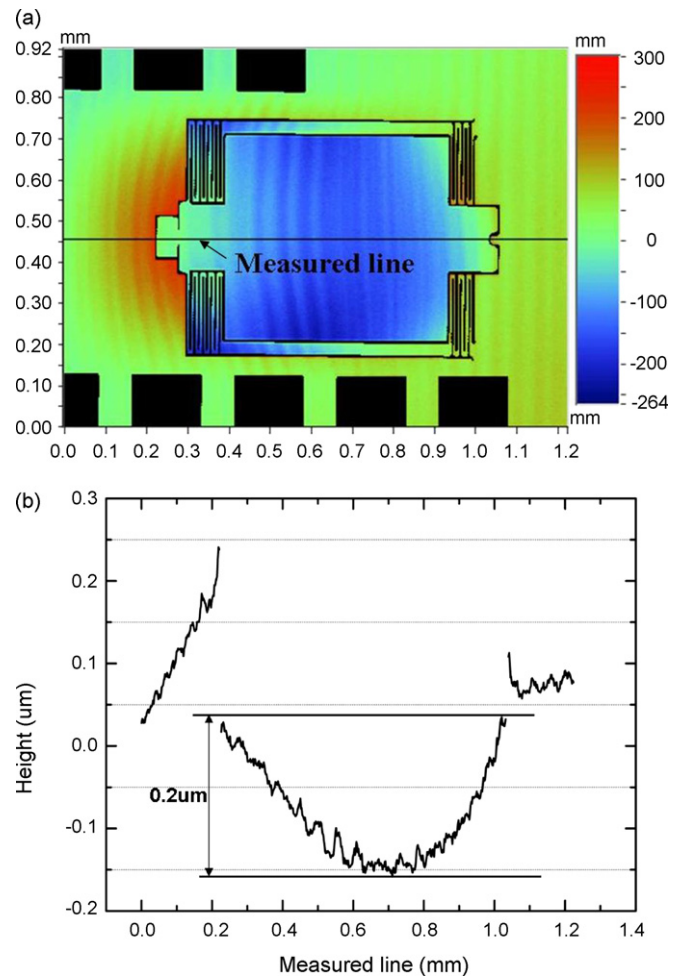


**Fig. 6.** The membrane bending measurement performed by using an optical 3D profiler: (a) The measured image of the optical 3D profiler (b) The height of the measured line.

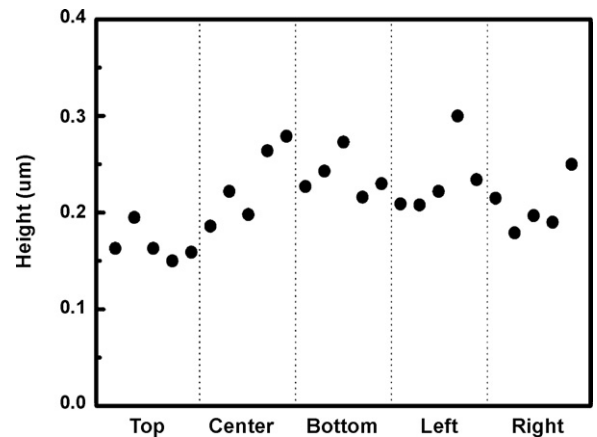


**Fig. 7.** The measured bending height of 25 randomly selected samples.

been found that 44% of the samples are within 0.2 μm bending range of height, and all the measured samples are within 0.3 μm bending height. From these measurements, it can be seen that this single crystalline bulk silicon structure is very effective for fabricating these flat membranes. Fig. 8 shows a SEM image of the fabricated switch, initially in the off-state. The crystalline bulk silicon mem-

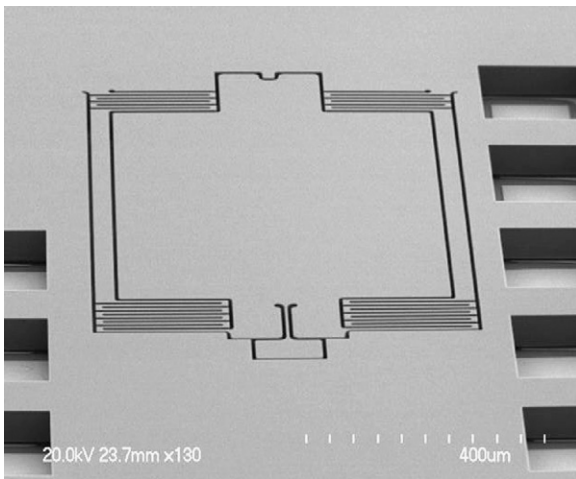


Fig. 8. A SEM image of the fabricated MEMS switch.

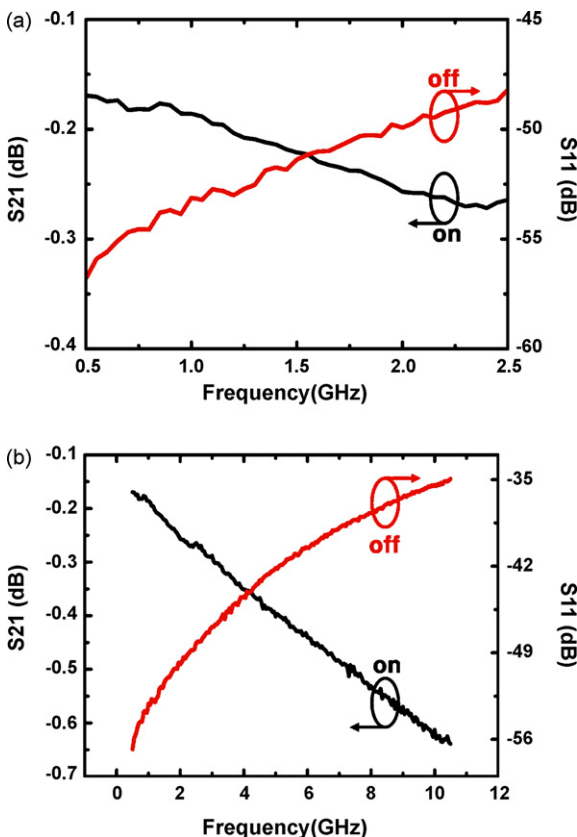


Fig. 9. RF characteristics of the fabricated MEMS switch: (a) narrow band, (b) wide band.

branes, and the folded springs for membrane actuation, are formed on the silicon wafer.

The measured S-parameters of the RF MEMS switch are shown in Fig. 9. The minimum actuation voltage is approximately 10–12 V; the isolation is around  $-50$  dB and the insertion loss is approximately  $-0.25$  dB at 2 GHz. The geometry of the pivot under the membrane, and the narrow gap between the electrode and flat membrane is a critical factor in achieving the low actuation voltage and good RF performance. Endeavors to reduce the operation voltages of the switches by optimizing the geometry design also have benefits in terms of the resulting reliability. Switches that can operate with lower voltages reduced the risk of charge accumula-

tion because the electric fields across the dielectric layer are lower, leading to reduced sticking problems. This design of switch also does not have to move as far, reducing any internal stresses caused by the motion of the switch [16].

#### 4. Conclusions

The design, fabrication, and characterization of a new concept for a low voltage actuated RF MEMS switch have been presented. This switch compensates for the weaknesses of the conventional seesaw and membrane types of switches. A low operation voltage has been achieved by means of designing a very uniform and well defined small gap between the electrodes and the membrane, using a flat silicon membrane and pivot with a seesaw mode operation design. Stiff single crystalline bulk silicon also reduces the bending of the membrane, and increases the reproducibility and reliability of fabricating the new switches.

The gap between the electrodes and the membrane is controlled by the depth of the etched glass wafer, rather than the sacrificial layer thickness. This method can avoid contamination, which can arise from the sacrificial layer residue, and can also secure the reliability of the contact metal.

The measured RF response has been found to be excellent, and shows that the new proposed RF switch is suitable for wireless components, or for space systems, where low power consumption is essential. The RF MEMS switch requires a hermetic package to preserve the microstructure and hence further study is proceeding with developing a wafer level chip scaling package.

#### Acknowledgements

This work was supported in part by the National Research Laboratory NRL, ROA-2007-000-20111-0 Program of the Ministry of Science and Technology Korea Science and Engineering Foundation.

#### References

- [1] B. Peng, W.L. Zhang, G.H. Chen, W.X. Zhang, H.C. Jiang, Modeling microwave behaviors of series cantilever MEMS switch, *Sensors and Actuators A* 125 (2) (2006) 471–476.
- [2] B.A. Centiner, J.Y. Qian, H.P. Chang, M. Bachman, G.P. Li, F.D. Flaviis, Monolithic integration of RF MEMS switches with a diversity antenna on PCB substrate, *IEEE Transaction on Microwave Theory and Techniques* 51 (1) (2003) 332–335.
- [3] C.L. Goldsmith, Z. Yao, S. Eshelman, D. Denniston, Performance of low loss RF MEMS capacitive switches, *IEEE Microwave and Guided Wave Letters* 8 (8) (1998) 269–271.
- [4] H. Yamazaki, T. Ikehashi, T. Ohguro, E. Ogawa, K. Kojima, K. Ishimaru, H. Ishiuchi, An intelligent bipolar actuation method with high stiction immunity for RF MEMS capacitive switches and variable capacitors, *Sensors and Actuators A* 139 (1–2) (2007) 233–236.
- [5] Z.J. Yao, S. Chen, S. Edelshen, C. Goldsmith, Micromachined low loss Microwave Switches, *IEEE Journal of Microelectro Mechanical Systems* 8 (2) (1999) 129–134.
- [6] J.B. Muldavin, G.M. Rebeiz, High isolation CPW MEMS shunt switches. Part 2. Design, *IEEE Transactions on Microwave Theory and Techniques* 48 (6) (2000) 1053–1056.
- [7] K. Rangra, B. Margesin, L. Lorenzelli, F. Giacomozzi, C. Collini, M. Zen, G. Soncini, L. Tin, R. Gaddi, Symmetric toggle switch – a new type of RF MEMS switch for telecommunication applications: design and fabrication, *Sensors and Actuators A* 123–124 (2005) 505–514.
- [8] T. Seki, Y. Uno, K. Narise, T. Masuda, K. Inoue, S. Sato, F. Sato, K. Imanaka, S. Sugiyama, Development of a large-force low loss metal contact RF MEMS switch, *Sensors and Actuators A* 132 (2) (2006) 683–688.
- [9] G.M. Rebeiz, *RF MEMS: Theory, Design and Technology*, John Wiley & Sons, Inc., New Jersey, USA, 2003.
- [10] J.S. Kim, Fabrication of flat RF MEMS switch membrane by minimizing of stress gradients in the Au membrane structure, in: *MRS Fall Meeting Proceedings* 741, 2002, pp. 87–91.
- [11] R.E. Strawser, K.D. Leedy, R. Cortez, J.L. Ebel, S.R. Dooley, C.F.H. Abell, V.M. Bright, Influence of metal stress on RF MEMS capacitive switches, *Sensors and Actuators A* 134 (2) (2007) 600–605.
- [12] E.P. Popov, *Introduction to Mechanics of Solids*, Prentice-Hall, New Jersey, USA, 1968.

- [13] J.E. Shigley, L.D. Mitchell, Mechanical Engineering Design, McGraw-Hill, USA, 1983.
- [14] J.S. Go, Y.H. Cho, Experimental evaluation of anodic bonding process based on the Taguchi analysis of interfacial fracture toughness, *Sensors and Actuators A* 73 (1–2) (1999) 52–57.
- [15] S.T. Lucic, J. Ames, B. Boardman, D. McIntyre, P. Jaramillo, L. Starr, M.H. Lim, Bond quality characterization of silicon-glass anodic bonding, *Sensors and Actuators A* 60 (1–3) (1997) 223–227.
- [16] C. Goldsmith, J. Ehmke, A. Malczewski, B. Pillans, S. Eshelman, Z. Yao, J. Brank, M. Eberly, Lifetime characterization of capacitive RF MEMS switches, in: *IEEE MTT-S International Microwave Symposium*, 1, 2001, pp. 227–230.

## Biographies

**Jong-Seok Kim** received the M.S degrees in electronic engineering from Kyungpook National University, Dae-Gu, Korea, in 2000, respectively. He then joined Nano Fab-

rication Center, Samsung Advanced Institute of Technology, Yong-In, Korea, where he developed process design and fabrication of micro devices. In 2006, he joined Display and Nanosystem Laboratory, College of Engineering, Korea University as a Ph.D course student. Since 2008, he is a senior engineer of DMC R&D center in Samsung Electronics. His research interests are in the area of design, fabrication, package of nano/micro device.

**Byeong-Kwon Ju** received the MS degree in electronics engineering from University of Seoul in 1988 and Ph.D degree in semiconductor engineering from Korea University in 1995. In 1988, he joined the Korea Institute of Science and Technology (KIST), Seoul, where he was engaged in development of mainly silicon micromachining and micro sensors as a Research Scientist. In 1996, he spent 6 months as a Visiting Research Fellow at Microelectronics Center, University of South Australia, Australia. Since 2005, he has been an associate professor of Korea University with his main interest in flexible electronics (OLED, OTFT), field emission device, MEMS (Bio and RF) and carbon nanotube-based nano systems.